

Modeling frost heave in silty soils

Varghese Babu^{1,*} and Dilip Gersappe^{1,**}

¹Department of Materials Science and Chemical Engineering, Stony Brook University, Stony Brook, NY 11794

Abstract. Crystallization of water in confinement differs significantly from its behavior in bulk. Depending on the size of the confinement, water can freeze at lower temperatures relative to the bulk freezing temperature. Crystallization in confinement also applies a pressure on the surrounding pore structure, called the crystallization pressure. This crystallization pressure is responsible for various phenomena ranging from damage caused by freezing thaw cycles in cement, salt crystallization in porous structures, and frost heave. Numerical modeling of crystallization in porous structures involves coupled modeling of liquid transport, its crystallization, and the interaction of the growing crystal with the surrounding pore structure. In this work, we build a model to study crystallization of water in silty soil with the aim of studying frost heave. We couple a Phase Field Model for ice crystallization with a Discrete Element Method to model the behavior of soil particles. Our results show that we can qualitatively capture the phenomenon of frost heave in silty soils.

1 Introduction

Ice formation in porous structures is a topic of significant interest due to its critical role in infrastructure applications, including soil mechanics [1] and cement durability [2]. For instance, frost heave is a phenomenon that occurs when water in the soil freezes, commonly observed in cold regions during winter. It causes portions of the soil to be pushed upward from the surface. Frost heave results from a combination of factors and is not primarily due to the expansion of water upon freezing, as the density change is relatively small compared to the magnitude of heaving observed. Furthermore, Taber [3] demonstrated that frost heave can also occur with benzene, which freezes with a decrease in volume. Rather, as the ground freezes, ice crystals form in some pores, creating a suction force that draws water from smaller, still unfrozen pores and even from the water table. This growing ice crystal exerts pressure on the surrounding pores, deforming them and eventually forming ice lenses much larger than the original pore dimensions [4, 5]. This process, known as ice segregation, is the primary driver of frost heave. Silty soils are particularly susceptible due to their small particle size, which leads to fine pores. Therefore, for frost heave to occur, two key conditions must be met: the soil must have small pores, and these pores must be connected to a water source.

The temperature at which water freezes in pores depends on the size of the pores [6]. According to Classical Nucleation Theory (CNT) for homogeneous crystallization, the size of the critical nucleus required for crystal growth depends on surface and bulk free energy. There is an energy penalty for creating interfaces, therefore, the

crystal has to be large enough such that the reduction in bulk free energy can compensate for the increase in interfacial free energy. As a result, in small pores, the crystal cannot be formed because of the relatively high surface-to-bulk ratio. In addition to the lower temperatures for crystallization, the crystal that forms inside the pore exerts a pressure on the pore structure, called the crystallization pressure. This is well studied in supersaturated salt solutions, and needs to be accounted for in models of frost heave. [7, 8]

Numerical studies of frost heave presents several challenges. The particle size of soil, 0.002mm or $2 \times 10^5 \text{\AA}$, when compared to a water molecule of radius 2.8\AA is very large. Therefore any direct simulation, like MD, even with coarse grained models of water, will be very expensive as one will have to simulate millions of water molecules. This disparity in length scales also extends to including soil mechanics into the models to account for the movement of the soil. Further, all this has to be coupled with both heat transfer and liquid transport in order to model the effects of the growing ice. Our approach here is to use a multi-scale approach, where we model the transport (both heat and liquid) using a meso-scale Lattice Boltzmann model (LBM). To model the ice formation we use a phase field model (PFM) that has been recast in the Lattice Boltzmann framework, and we couple all these approaches with a Discrete Element Model (DEM) to model the soil mechanics. We could solve the PFM with conventional finite-element methods, however we intend to model flow of water through the porous medium in the future and hence we chose LBM for solving PFM.

*e-mail: varghese.babu@stonybrook.edu

**e-mail: dilip.gersappe@stonybrook.edu

2 Models and Methods

2.1 Phase Field Model

Phase Field Models are a method to track an interface between two phases. We describe the phase in the system using the phase field function $\phi(\mathbf{x})$, where \mathbf{x} is a position in the system. For crystallization, the system has two phases, solid and liquid which are described by $\phi = 1$ and $\phi = -1$ respectively. The region with phase value between -1 and 1 represents the interface of the region. The evolution of the phase field is defined by a free energy functional $\mathcal{F}(\phi, \nabla\phi)$ which depends both on the phase field function and its gradient. The evolution of ϕ is described by the Allen-Cahn equation if ϕ is not conserved and is described by the Cahn-Hilliard equation if it is conserved [9]. For a conserved order parameter the time derivative must satisfy a continuity equation, which is not a constraint we have here. The differential equation for the evolution of ϕ is

$$\frac{\partial\phi}{\partial t} = -L \frac{\delta\mathcal{F}}{\delta\phi} \quad (1)$$

where $\frac{\delta\mathcal{F}}{\delta\phi}$ is the functional derivative.

In this project, we define two functions - $\phi(\mathbf{x})$ to indicate the phase value at \mathbf{x} and $\theta(\mathbf{x})$ which indicates the temperature at \mathbf{x} . We define the free energy functional as

$$\mathcal{F}(\phi, \theta) = \int \left(\frac{1}{2} \frac{W_0^2}{\tau} |\nabla\phi|^2 + \overbrace{\frac{1}{4}(1 - \phi^2)^2 + \lambda\theta G(\phi)}^f \right) d\mathbf{x} \quad (2)$$

where $G(\phi) = \frac{1}{5}\phi^5 - \frac{2}{3}\phi^3 + \phi$ with derivative $G'(\phi) = (1 - \phi^2)^2$. $\frac{W_0^2}{\tau}$ is a quantity related to the interfacial free energy between ice and water. θ is the dimensionless temperature defined by $\theta = \frac{C_p(T(\mathbf{x},t) - T_m)}{L}$ where C_p is the heat capacity at constant pressure and L is the latent heat of fusion. θ is also defined by a differential equation.

The differential equations that define the evolution of ϕ are derived from Eq. 1 with $L = 1$, the functional derivative is given by $\frac{\delta\mathcal{F}}{\delta\phi} = \frac{\partial f}{\partial\phi} - \frac{W_0^2}{\tau} \nabla^2\phi$,

$$\frac{\partial\phi}{\partial t} = \frac{W_0^2}{\tau} \nabla^2\phi + (\phi - \phi^3) - \lambda\theta(1 - \phi^2)^2 \quad (3)$$

$$\frac{\partial\theta}{\partial t} = \kappa \nabla^2\theta + \frac{1}{2} \frac{\partial\phi}{\partial t} \quad (4)$$

The temperature variable θ evolves according to Eq. 4, with a source term originating from the latent heat due to crystallization. Now we describe how these variables relate to various physical quantities. This system is defined by W_0, τ, κ and λ . Following [10], we have

$$d_0 = a_1 \frac{W_0}{\lambda} \quad (5)$$

and

$$\beta = a_1 \left[\frac{\tau}{\lambda W_0} - a_2 \frac{W_0}{\kappa} \right] \quad (6)$$

where

$$d_0 = \frac{\gamma_0 T_m C_p}{L^2} \quad (7)$$

is the ‘‘thermal capillary length’’ which relates to the change in temperature across a curved interface as given by Gibbs-Thomson equation and β is the kinetic coefficient. Following [11–13] we will set $\beta = 0$. For the present study $a_1 = 5\sqrt{2}/8$ and $a_2 \approx 0.6267$ [11]. Plugging in the following values

$$\begin{aligned} \gamma_0 &= 2.845 \times 10^{-2} Jm^{-2} \\ C_p &= 4.23 \times 10^6 Jm^{-3}K^{-1} \\ T_m &= 276.9K \\ L &= 1.12 \times 10^8 Jm^{-3} \end{aligned}$$

into Eq. 7, we get $d_0 = 2.66 \times 10^{-9}m$ [14, 15]. Following [11] we fix $\beta = 0$ by choosing $\lambda = \frac{\tau\kappa}{a_2 W_0^2}$. We introduce δ_x and δ_t as our conversion factors to simulation units, i.e 1 unit in the simulation is δ_x in SI. We fix $W_0 = \delta_x$ and $\tau = \delta_t$ and $\kappa = 4 \frac{\delta_x^2}{\delta_t}$, then $\lambda = 6.3826$. From Eq. 5, we get, $d_0 = \frac{0.8839\delta_x}{6.3826} = 0.138\delta_x$ which fixes $\delta_x \approx 1.91 \times 10^{-8}m$. Using $\kappa = 4 \frac{\delta_x^2}{\delta_t}$, with $\kappa = 0.1 \frac{mm^2}{s} = 10^{-7}m^2/s$, which makes $\delta_t = 1.5 \times 10^{-8}s$. We have discussed the values for δ_x and δ_t to show how these can be computed. Although these values correspond to experimental observations of water crystallization, in this project, we focus on demonstration of our numerical technique. Therefore, to ease our computational effort we use a much reduced $d_0 = 10^{-6}m$ and the other values are correspondingly different.

We solve these partial differential equations using the Lattice Boltzmann equations. Using LBM-like update equations to solve differential equations is discussed in various works referred here [11–13].

2.2 DEM simulation

In this section, we discuss the Discrete Element Method (DEM) simulations we have used to simulate silt. We simulate a polydisperse packing of $N = 3000$ spheres interacting via linear normal contact and tangential friction. The parameters characterizing the particle-particle interactions are shown in Table. 1. The size distribution of the grains is shown in Fig. 1a. We calibrate our model with an existing study of silt [16]. We use uniaxial compression of the DEM model and measure the deviator stress, $q = \sigma_1 - \sigma_3$ and the mean stress, $p = (\sigma_1 + 2\sigma_3)/2$ where $\sigma_1, \sigma_2 = \sigma_3$ are the three components of the stress tensor. The direction 1 corresponds to the axis along which we compress, which in our case is the z axis. The results are shown in Fig. 1c. In addition we also show the evolution of voidratio Fig. 1d and results of direct shear of our sample Fig. 1b. Our objective here is not to calibrate the DEM sample with experimental results, but to show that the DEM sample behaves reasonably under various tests. We will refine the parameters to characterize a real specimen in future studies.

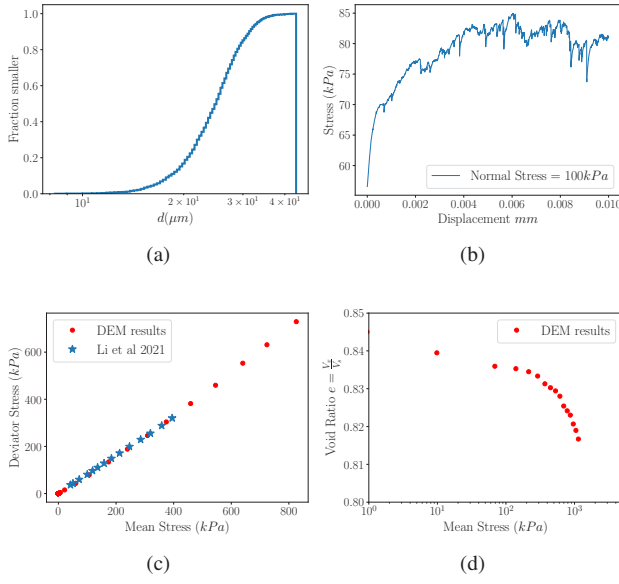


Figure 1: **a)** Size distribution of grains. **b)** Direct shear of the sample. **c)** Uniaxial compression of the DEM sample compared with DEM studies from existing literature of silt [16]. **d)** Evolution of void ratio of the sample under uniaxial compression.

	SI units
Average Diameter of the particle d	$2.5 \times 10^{-5} m$
Density ρ	$2203 kg/m^3$
Acceleration due to gravity g	$9.8 m/s$
k_n	$\frac{\pi R^2}{2R} 800 MPa$
Coefficient of restitution	0.69
Poisson ratio ν	0.17

Table 1: Table with values for simulation

2.3 DEM-Crystal Phase interaction

We use an alpha shape (a generalization of convex hull) to capture the shape of the crystal phase and this alpha shape is written to a STL file using CGAL library [17]. LAMMPS can read the STL file and replace it with a collection of spheres. A crystal particle and a soil particle are neighbors if $r_{ij} < R_i + R_j + \epsilon$ where r_{ij} is the distance between the centers of the particles and R_i, R_j are radii of the two particles. $\epsilon = 0.8\sigma$ where σ is the average diameter of the polydisperse soil packing. Each soil particle i will have N_i crystal particles as neighbors. We compute $\hat{n} = \sum_j^{N_i} \hat{n}'_j$ where \hat{n}'_j is the normal connecting the sphere i to neighbor j .

The magnitude of the repulsive force acting of the soil particle along \hat{n} is defined by the potential $V(r) = A(1 - \frac{r}{\epsilon})^2$ where A is a parameter and $r = r_{ij} - (R_i + R_j)$. The value we have chosen for A is 5×10^{-6} . This is an approximation for the crystallization pressure.

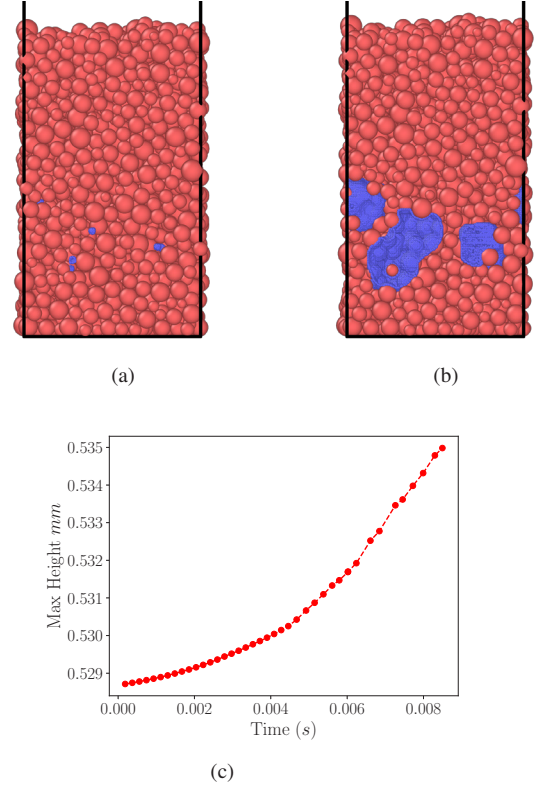


Figure 2: **a)-b)** Snapshots from LBM+DEM simulation. We obtain qualitative observation of the frost heave phenomena using the numerical procedure. Red-Soil particles, Blue-Crystal. **c)** Frost heave as measured by the heights z coordinate of among the particles plotted against time.

3 Implementation and results

3.1 Implementation.

3.1.1 LBM-DEM integration

The dimensions of the region we simulate in LAMMPS is $L_x = L_y = \frac{2}{3}L_z \approx 3 \times 10^{-4} m$.

We use Lattice Boltzmann implemented in OpenLB to solve the phase field and LAMMPS to simulate the interaction between soil and the ice crystal. We first generate the soil structure. In LAMMPS, we generate $N = 3000$ particles with size distribution as shown in Fig. 1a and settle them under gravity. This packing of spheres is considered as the soil sample. We initialize this sphere packing in OpenLB as regions with bounce back boundary condition for the phase field equation. This is followed by identification of the void regions in the soil sample - we identify a void as an empty space where we can insert a particle of $\frac{1}{2}\sigma$ radius. We identify n such void spaces and initialize the ice nuclei as $\phi(\mathbf{x}, t) = \tanh(\frac{r - |\mathbf{x} - \mathbf{x}_0|}{d_0})$ where \mathbf{x}_0 is located in a void space and $r = \frac{1}{2}\sigma$ is a parameter which determines the size of the initial crystal. The heat equation is initialized as a uniform undercooling of $\Delta \approx -26^\circ C$ throughout the system. After initialization we evolve the

heat equation and the phase field equation using the lattice Boltzmann method for ΔT_{PFM} time. Now we perform DEM simulation, which includes the added interaction between crystal and soil particles, until the kinetic energy in the system decays to a small number, thereby indicating that the system has settled down. We read the new particle positions as the new boundary conditions for LBM in OpenLB and the process repeats till the desired number of time steps.

3.2 Results

As shown in Fig. 2 a-b-c, the numerical method qualitatively captures the behavior of frost heaving. Fig. a is the snapshot of the system at $T = 0$ and Fig. b is at $T = 0.008298$. Fig. c shows the evolution of the height of the soil sample between the two snapshots. We quantify frost heave by measuring the maximum z coordinate among all the soil particles, and the results are shown in Fig. 2 c. The growing crystal interacts with the soil particles to push the soil upwards. We also note that our methodology captures merging of ice-nuclei and the interaction with soil particles. This method should naturally account for the shape of ice lenses as, once we apply a constant pressure in the z direction, it will be easier to deform the soil sample along in the $x - y$ plane and therefore the nuclei will expand in the $x - y$ plane.

4 Conclusions and Future Work

We have successfully integrated OpenLB with LAMMPS to enable DEM+PFM calculations. Using our numerical formulation we have qualitatively observed frost heave. To accurately model the phenomenon, we need several modifications. There needs to be an accurate way to characterize the interaction between the soil and the ice crystal, which corresponds to a given value of crystallization pressure and we also need to account for the flow of water from the reservoir to the ice crystal to account for the cryosuction. Our current work opens up the possibility of extending this method with continuum models like Lattice Spring Model for simulating the soil.

5 Acknowledgements

This project is supported by the United States Army Corps of Engineers, Engineer Research and Development Center's Cold Regions Research and Engineering Laboratory (ERDC-CRREL, Contract No. W913E524C0009) program. Any opinions, findings and conclusions or recommendations expressed in this material are those of the author(s) and do not necessarily reflect the views of the Broad Agency Announcement Program and ERDC-CRREL.

References

[1] S.S. Peppin, R.W. Style, The physics of frost heave and ice-lens growth, **12**, 1 (2013).

[2] X. Zhu, M. Vandamme, Z. Jiang, L. Brochard, Molecular simulation of the confined crystallization of ice in cement nanopore, **159**, 154704 (2023-10-21).

[3] P.B. Black, M.J. Hardenberg, Historical Perspectives in Frost Heave Research: The Early Works of S. Taber and G. Beskow (CRREL, 1991)

[4] D.D. Xia, Frost heave studies using digital photographic technique (2006), <https://era.library.ualberta.ca/items/ee29789b-127c-4b01-ab89-e8b9d43c4023>

[5] J. Torrance, T. Elliot, R. Martin, R. Heck, X-ray computed tomography of frozen soil, **53**, 75 (2008-06). [10.1016/j.coldregions.2007.04.010](https://doi.org/10.1016/j.coldregions.2007.04.010)

[6] G.H. Findenegg, S. Jähnert, D. Akcakayiran, A. Schreiber, Freezing and melting of water confined in silica nanopores, *ChemPhysChem* **9**, 2651 (2008).

[7] M. Steiger, Crystal growth in porous materials—I: The crystallization pressure of large crystals, **282**, 455 (2005-09). [10.1016/j.jcryspro.2005.05.007](https://doi.org/10.1016/j.jcryspro.2005.05.007)

[8] J. Desarnaud, D. Bonn, N. Shahidzadeh, The Pressure induced by salt crystallization in confinement, **6**, 30856 (2016-08-05). [10.1038/srep30856](https://doi.org/10.1038/srep30856)

[9] N. Provatas, K. Elder, *Phase-Field Methods in Materials Science and Engineering* (John Wiley & Sons, 2011)

[10] A. Karma, W.J. Rappel, Quantitative phase-field modeling of dendritic growth in two and three dimensions, **57**, 4323 (1998-04-01). [10.1103/PhysRevE.57.4323](https://doi.org/10.1103/PhysRevE.57.4323)

[11] A. Cartalade, A. Younsi, M. Plapp, Lattice Boltzmann simulations of 3D crystal growth: Numerical schemes for a phase-field model with anti-trapping current, **71**, 1784 (2016).

[12] A. Younsi, A. Cartalade, On anisotropy function in crystal growth simulations using Lattice Boltzmann equation, **325**, 1 (2016-11), 1606.09432. [10.1016/j.jcp.2016.08.014](https://doi.org/10.1016/j.jcp.2016.08.014)

[13] Q. Tan, S.A. Hosseini, A. Seidel-Morgenstern, D. Thévenin, H. Lorenz, Modeling ice crystal growth using the lattice Boltzmann method, **34**, 013311 (2022-01-01), 2101.07163. [10.1063/5.0072542](https://doi.org/10.1063/5.0072542)

[14] A. Galfré, X. Huang, F. Couenne, C. Cogné, The phase field method—From fundamentals to practical applications in crystal growth, **620**, 127334 (2023-10). [10.1016/j.jcryspro.2023.127334](https://doi.org/10.1016/j.jcryspro.2023.127334)

[15] Y. Zhang, J. Khodadadi, Ice-water interfacial energy between 235.35 and 237.15 K deduced from homogeneous nucleation rate, **16**, 534 (2016-05). [10.1016/j.cap.2016.02.006](https://doi.org/10.1016/j.cap.2016.02.006)

[16] T. Li, M. Jiang, L. Li, Dem analysis of mechanical behavior of unsaturated silt under strain-controlled constant stress ratio compression tests, *International Journal of Geomechanics* **21**, 04021197 (2021).

[17] T.K.F. Da, S. Lorient, M. Yvinec, in *CGAL User and Reference Manual* (CGAL Editorial Board, 2024), 6th edn., <https://doc.cgal.org/6.0.1/Manual/packages.html#PkgAlphaShapes3>